JOURNAL OF GEOPHYSICAL RESEARCH, VOL. 115, A02207, doi:10.1029/2009JA014572, 2010

Click Here for Full Article

Stepwise feature of aurora during substorm expansion compared with the near-Earth tail dipolarization: Possible types of substorm dynamics

M. H. Saito,[1] Y. Miyashita,[2] M. Fujimoto,[3] K. Liou,[4] Y. Saito,[3] and J. B. Sigwarth[5]

Received 15 June 2009; revised 30 August 2009; accepted 9 September 2009; published 12 February 2010.

[1] Previous studies of auroral behaviors have suggested that the substorm expansion is a result of a chain of processes originating in the magnetotail. We present a detailed study on the substorm expansion behavior on 3 November 1998, using the global auroral images from Polar and the conjugate central plasma sheet data from Geotail in the near-Earth tail. The closer inspection of the auroral data enables us to characterize the stepwise feature of the auroral evolution, which were found to be spatially and temporally separable into two intense auroral activities: the initial brightening of the substorm arc and the second aurora that took place eastward of the first one with the time delay of 4.5 min. Comparing the near-Earth tail observation of the fast plasma flow, we show that the observed time lag of 4.5 min can be explained by a systematic chain of plasma processes in the central plasma sheet, indicating that this time delay can be interpreted as a generic behavior. The generality of the stepwise evolution within the expected time lag of 2–6 min is also pursued, and is found for three out of six substorms. With respect to the stepwise feature, our observation of six substorms suggests that there are at least three types of substorm expansion dynamics that are attributable to different chains of tail processes.

Citation: Saito, M. H., Y. Miyashita, M. Fujimoto, K. Liou, Y. Saito, and J. B. Sigwarth (2010), Stepwise feature of aurora during substorm expansion compared with the near-Earth tail dipolarization: Possible types of substorm dynamics, *J. Geophys. Res.*, *115*, A02207, doi:10.1029/2009JA014572.

1. Introduction

[2] Auroral behavior during a substorm has been extensively studied and has led to many implications for magnetospheric dynamics [e.g., *Elphinstone et al.*, 1996], though the corresponding plasma processes inside the plasma sheet are far from understood definitively. The rough picture of a substorm is that it is an explosive phenomenon that consists of slow energy storage processes and fast energy release processes of the magnetosphere. At substorm expansion phase onset (substorm onset), an auroral arc shows sudden intensification, or brightening, in a spatially localized region. An auroral bulge is a bunch of thin auroral arcs that include both small-scale and large-scale structures. During the substorm expansion phase, the auroral bulge evolves systematically. Soon after the substorm onset, the spatial extent of the auroral bulge increases and expands globally. Note that this auroral bulge evolution is neither continuous nor homogeneous.

[3] Many auroral observations have suggested that auroral evolutions show stepwise features and that substorm expansion might have several stages to evolve. *Sergeev and Yahnin* [1979] studied the features of auroral bulge evolutions during substorms using all-sky cameras from several dense arrays of stations and they suggested that the following features seem to be common: Initially localized bulges arise and expand with new bright arc formations developing. They also commented that similar descriptions of these features can be found in previous published works [*Akasofu*, 1964, 1965, 1972; *Lassen et al.*, 1974; *Oguti*, 1975]. The stepwise feature was also confirmed on the basis of space-borne experiments of auroral substorms [*Craven et al.*, 1989]. The stepwise feature has also been noted in ground-based magnetic field observations: The behavior of the magnetic bay may correspond to a sudden poleward shift of the auroral electrojet (see *Hones* [1985] and introduction therein). *Hones* [1985] proposed that the sudden poleward shift of the aurora is the manifestation of the thickening of the plasma sheet and the retreat of the neutral line in the plasma sheet. As he discussed in his paper, the stepwise feature is difficult to put the phenomena into a morphological substorm model, since it is possible to recognize this kind of phenomenon as an occurrence of a new substorm. Other researchers describe this stepwise behavior of the auroral emergence as the onset

[1]Institute of Space Science, National Central University, Jhongli, Taiwan.
[2]Solar-Terrestrial Environment Laboratory, Nagoya University, Nagoya, Japan.
[3]Institute of Space and Astronautical Science, Japan Aerospace Exploration Agency, Sagamihara, Japan.
[4]Johns Hopkins University Applied Physics Laboratory, Laurel, Maryland, USA.
[5]NASA Goddard Space Flight Center, Greenbelt, Maryland, USA.

Copyright 2010 by the American Geophysical Union.
0148-0227/10/2009JA014572$09.00

of full expansion. In order to understand this behavior better, it is important to find a counterpart phenomenon inside the plasma sheet to determine the physics behind this stepwise feature.

[4] Recently, *Kadokura et al.* [2002] presented a detailed analysis of a substorm event using UV imager onboard the Akebono satellite and also pointed out that the stepwise feature might be common. They tried to explain the stepwise feature of the auroral bulge evolution in the context of magnetotail dynamics. The knowledge of auroral behaviors has been accumulated, and it is desirable to combine these behaviors with substorm phenomenology from the magnetospheric observations. There are, however, many difficulties: One is that these features of aurora and tail observations are usually presented with rather qualitative descriptions. In addition to that, there is the problem or question of generality of the examined auroral substorms. The definition of bulge itself also varies between researchers and between substorm events, since no two substorm activities are alike. Due to the complex nature of the aurora, the relationship between the auroral behaviors and the tail dynamics are largely unknown.

[5] *Friedrich et al.* [2001] carried out a systematic examination of the temporal evolution of the poleward border of the auroral emissions of 557.7 nm and 630.0 nm lines during early substorm expansion phases. They established the chronology of the stepwise auroral evolution using the fact that the emission lines (557.7 nm and 630.0 nm) as seen by the CANOPUS meridian scanning photometers initiate their poleward motions at progressively different times. They found that there was a time delay between the rapid motion of the poleward boundaries of the two emission lines. The typical time delay was found to be 1–5 min, and can be interpreted as a generic feature of substorm dynamics. Since 630.0 nm emission can provide the location of polar cap boundary [*Blanchard et al.*, 1995], one can interpret this timing as the indication of the lobe magnetic reconnection [*Blanchard et al.*, 1997]. On the other hand, 577.7 nm emission line can provide the onset timings of near-Earth tail disturbances [*Samson et al.*, 1992]. On the basis of these auroral phenomena as a diagnosis of the magnetosphere dynamics, the interpretation of this time delay was presented by *Friedrich et al.* [2001] in terms of magnetospheric dynamics. The observed time delay of 1–5 min implied the presence of fast mode waves that can propagate to the midtail region through the central plasma sheet. In their scenario, the fast mode wave is generated in the near-Earth tail and functions as a trigger of the magnetic reconnection in the midtail. However, the phenomenology of the magnetotail dynamics at substorm onset is a disputable topic (see section 3). The question whether the stepwise auroral evolution is relevant to tail dynamics is also unclear and has not been observationally confirmed.

[6] In this paper, the stepwise feature of auroral evolution is of particular interest, and will be shown with the detailed spatial and temporal characteristics from global auroral imagers. The direct measurements of tailward propagating fast mode wave were recently identified [*Saito et al.*, 2008a] for the substorm on 3 November 1998 in which Geotail was located in the central plasma sheet at $X_{GSM} = -12\ R_E$. The aim of this study is to reveal the relationship between auroral activity and the magnetospheric dynamics by comparing substorm expansion phase aurora from the global imagers with the concurrent central plasma sheet data in the near-Earth tail. In section 2, we will present the observations that demonstrate the stepwise feature of auroral evolution and the concurrent tail signatures of fast flow and dipolarization, using six substorm events including the event on 3 November 1998. In section 3, we will combine the signatures presented in this study and our previous findings of the low-frequency waves that appeared at the dipolarization onset [*Saito et al.*, 2008a; *Saito et al.*, 2008b] into one scenario. A brief review of conventional substorm initiation models, namely, near-Earth neutral line model (NENL) and the current disruption (CD) model, will be given and will be evaluated. We will discuss that our observations basically provide strong support for the chain of processes in the central plasma sheet suggested by *Friedrich et al.* [2001]. However, we will also suggest that there are other types of auroral substorms that have different chains of plasma processes inside the plasma sheet. In section 4, our conclusions with respect to the stepwise features of substorm expansion will be summarized.

2. Observations

[7] The near-Earth tail observation from the central plasma sheet is necessary to examine a temporal behavior of the fast earthward flows. The previous study of the fast earthward flow from the off-central plasma sheet [*Hones et al.*, 1976; *Angelopoulos et al.*, 1996] showed some time delay for spacecraft to detect the flow, which was interpreted that the spacecraft became able to detect the fast flow when a significant thickening of the plasma sheet occurred after a substorm expansion phase onset.

[8] In the Geotail data set we have found six intervals of dipolarizations detected in the vicinity of the magnetic equator of the near-Earth tail ($X_{GSM} \sim -10\ R_E$) that have the concurrent auroral images from Polar [*Saito et al.*, 2008b]. The uniqueness of these events is that Geotail was located in the vicinity of the magnetic equator ($|B_x| < 10$ nT) continuously before the dipolarization onset. We use magnetic field data [*Kokubun et al.*, 1994] and ion velocity moment data [*Mukai et al.*, 1994] to examine tail signatures of dipolarization and fast flows. The relative longitudinal locations of Geotail can be mapped to the ionosphere using the T96 model [*Tsyganenko*, 1995]. The auroral data were provided by the visible imaging system (VIS) [*Frank et al.*, 1995] and ultraviolet imager (UVI) [*Torr et al.*, 1995] onboard Polar. Both imagers, VIS and UVI, are capable of obtaining the two-dimensional global images of auroral activity with a spatial resolution of ~50 km, and were operating for the substorm event on 3 November 1998. We monitor onset aurora (usually known as an initial auroral brightening or an auroral breakup that is generally considered as an indicator for substorm onset) and the subsequent auroral activities. Then, the auroral activation timings and locations are compared with the near-Earth tail observations.

[9] The following section consists of two parts: the first part is to demonstrate the stepwise feature of the aurora and a method to compare the auroral behavior with the near-Earth tail data using the event on 3 November 1998; the second part is to present the analysis result for all six events.

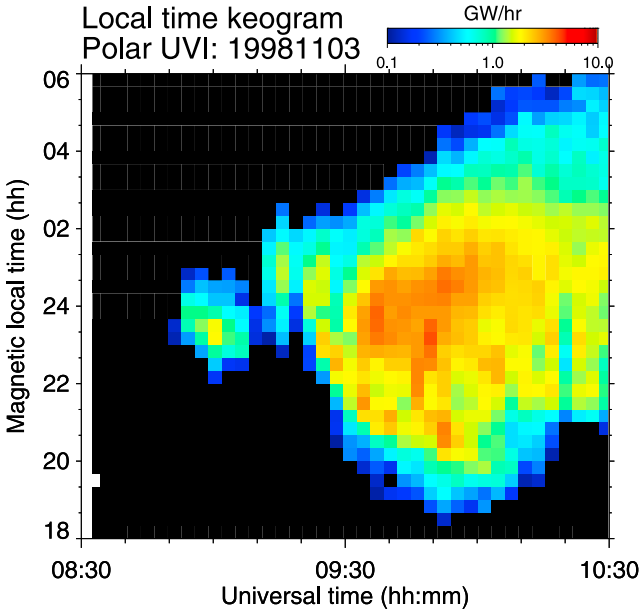

Figure 1. Magnetic local time keogram of the substorm on 3 November 1998 in ultraviolet N_2 Lyman–Birge–Hopfield Longer wavelength (LBHL) emissions of aurora.

2.1. Substorm on 3 November 1998

[10] Figure 1 is a magnetic local time keogram constructed from the Polar UVI data, showing the auroral substorm activity on 3 November 1998 from 0830 universal time (UT) to 1030 UT. The term "keogram" is usually referred to the time series of the north–south slit of the ground-based all-sky auroral camera. Since the spacecraft-borne auroral imager from the Polar UVI is capable of obtaining a wide range of the nightside aurora, the magnetic local time keogram can be constructed [*Meng and Liou*, 2002]. In Figure 1, the color represents the integrated auroral intensities over the magnetic latitudes (Mlats). The azimuthal extent of the activity is easily seen. The major auroral activation at 0924 UT at ~23 h magnetic local time (MLT) is the main interest of this study (the detailed timings will be shown in Figure 2). Before this time, there were two minor auroral activities that occurred at 0853 UT and at 0912 UT. This kind of auroral activity seems to be common and observed for other substorms [e.g., *Voronkov et al.*, 2003]. In this study, we do not focus on these minor auroral activities, but focus on the major expanding behavior after 0924 UT. These minor auroral activities failed to expand globally, while the major auroral activation expanded globally. Note that the expansion behavior of the aurora after 0924 UT is not continuous in space and time. The intense auroral activity

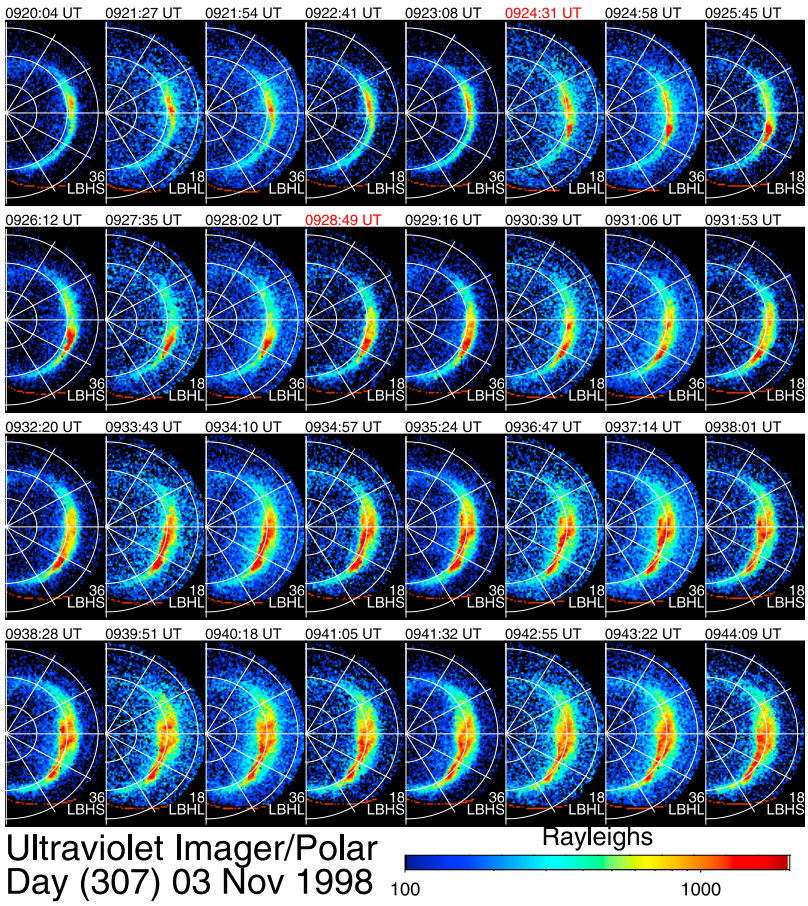

Figure 2. A sequence of nightside auroral images in the N_2 Lyman–Birge–Hopfield (LBH) bands with the exposure time of 18 and 36 s from Polar ultraviolet imager on 3 November 1998. The first aurora activation (snapshot labeled 0924:31 UT in red) and the second aurora activation (snapshot labeled 0928:49 UT in red) are shown.

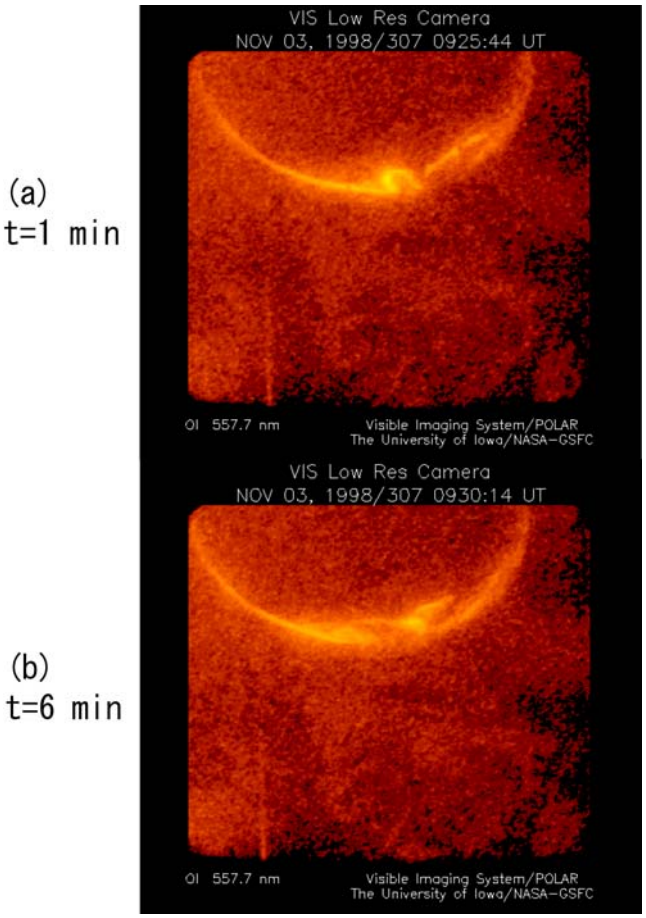

Figure 3. Auroral images from Polar VIS at the substorm onset on 3 November 1998.

at 0924 UT at ~23 h MLT moved westward, while another intense aurora appeared at 0930 UT at ~24 h MLT. In this study, we call this kind of two-stage behavior stepwise.

[11] With the use of global images, an emergence of intense aurora is seen as a spot in an image. We can pick two onset timings for the first and second auroras, where the first and the second are determined according to their chronological order of emergence. Our definitions of the first aurora and the second aurora are different from those two timings studied by *Friedrich et al.* [2001]. While they focused on the poleward border of the aurora from the ground, we focus on the intense aurora that can be well determined in the global imager data. The ground-based auroral photometers are capable of detecting weaker aurora, the poleward border can be reliably measured. Here the space-based global auroral imagers are suitable for examining intense auroral activities. However, the wide spatial view of the images allows us to examine the stepwise feature of aurora in a different way from the ground-based observations. Detailed determination of the first and second auroras is given below.

[12] Figure 2 is the time series data of snap shots taken from the Polar UVI from 0920 UT to 0944 UT on 3 November 1998, showing the auroral activity on the nightside of the northern hemisphere. The format is given by the Mlat and the magnetic local time, which are based on the Altitude Adjusted Corrected Geomagnetic Coordinates (AACGM) [*Baker and Wing*, 1989]. The first aurora (initial brightening of substorm) is seen in the snap shot labeled at 0924:31 UT. The time tag is the center of the camera exposure time (either 18.4 s or 36.8 s); this can be seen in each image by numbers 18 or 36. The image tagged as 0923:08 UT had 36.8 s exposure time from 0922:50 to 0923:26 UT. The initial brightening is seen in an image tagged 0924:31 UT (indicated by red color) with the exposure time of 18.4 s. Hence the substorm onset occurred after 0923:26 UT and before 0924:40 UT. The center of this interval 74 s is 0924:03 UT. In this study, we take that the substorm onset time is the center of the expected interval for the initial brightening onset. The estimated onset time for the substorm on 3 November 1998 is now written as 0924:03 UT ±37 s. The error comes from the duration of the expected time interval, which means that the onset time (the center of the interval) does not mean the most probable onset timing, but just the center of the expected time interval for the initiation of the substorm expansion phase. The snap shot at 0930:39 UT shows the second auroral onset. Likewise the onset time for the second aurora was found to be 0928:39 UT ±19 s. Hence, the time lag (delay) between the first and the second auroras was found to be 4.5 min. The location of the second auroral onset was eastward of the first auroral onset and was separated by 1 h. The second aurora is also seen as a discrete spot in the image. Both the first and second auroras are separable, since the discrete spots are seen in the images. Both the first and second auroras started in a localized region. The location (magnetic latitude, MLT) of the first auroral onset was given as (68°, 22.8 h MLT), while that of the second auroral onset was (70°, 23.8 h). The latitudinal separation in the ionosphere is ~2°. The second auroral onset was located northward (i.e., poleward) of the first auroral activity.

[13] Figure 3 shows auroral images in 557.7 nm emission just after the substorm onsets. The exposure time for the images was 44 s. In both Figures 3a and 3b, a globally distributed quiet oval and some intense aurora are seen. Figure 3a is the image data taken at 0925 UT on 3 November 1998 (t = 1 min, where t = 0 is the first aurora onset time determined from Polar UVI), showing the fine spatial structure of the first aurora. Likewise, Figure 3b is the image data taken at 0930 UT (t = 6 min), which is approximately 6 min after the first aurora onset and approximately 2 min after the second aurora onset. Both the first and second auroras onsets were characterized by localized intense aurora. These two auroras had spatial structures that differ from each other, suggesting different tail dynamics responsible for their generations.

[14] The first aurora has the spatial structure such that the auroral arc in the onset region was elongated poleward with increased intensity. This elongated arc was tilted toward the west. From Figures 1 and 2, we can see that this localized auroral intensification moved westward after the substorm onset. Eastward of the first aurora, there was slightly intensified auroral structure that was located poleward of the global quiet oval. This eastside structure is a remnant of the previous localized minor auroral activity. The intensity of this auroral activity in the eastside became weaker and disappeared by 0927 UT, as seen in Figure 2.

[15] The second aurora intensified locally again in the center of the onset region with extended arc structures on

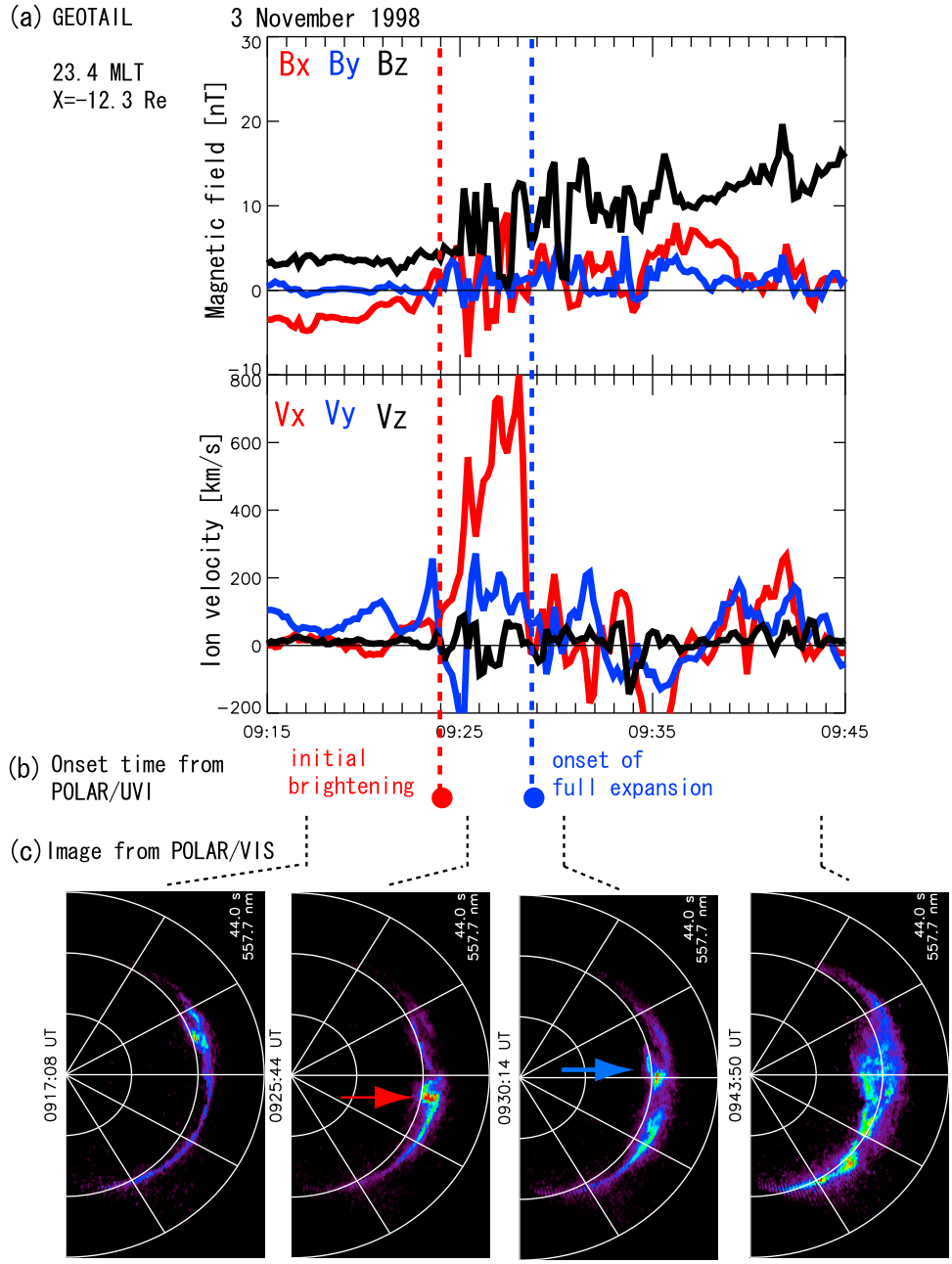

Figure 4. (a) Geotail observations on 3 November 1998 in the vicinity of the magnetic equator of the near-Earth tail. The magnetic field data, B_x, B_y, and B_z, and the ion velocity data, V_x, V_y, and V_z, are plotted for 30 min. (b) Timings of the first and the second aurora determined by Polar UVI. (c) Images of the aurora from Polar VIS in the visible light spectrum (in 557.7 nm emissions) in the AACGM coordinate system. A red arrow and a blue arrow show the commencement timings of the first aurora (the initial brightening) and the second aurora (the onset of the full expansion), respectively.

both sides of the most intensified region. These arc structures were located distinctly poleward of the quiet oval. Likewise, the most intensified region at the center was located poleward of the quiet oval.

[16] Figure 4 shows the Geotail observation from the near-Earth tail at the substorm onset on 3 November 1998. The magnetic local time of the Geotail spacecraft was 23.4 h MLT, according to the T96 model. The azimuthal location of Geotail was close to both the first and second auroras onset locations. The azimuthal separations between the Geotail spacecraft and these auroras were found to be 0.6 h for the first aurora and 0.4 h for the second aurora. At the radial distance of 12.4 R_E, the Geotail spacecraft and both auroral activations were azimuthally separated by the distance of ~1.5 R_E.

[17] Geotail data showed the signature of the magnetic dipolarization and the fast earthward flow. In the vicinity of the magnetic equator, the dipolarization was observed as an increase of B_z components. The fast earthward flow of ions was observed as a transient increase of the V_x com-

Table 1. Characteristics of the First and Second Aurora Onsets Determined in This Study

Events	Date (yymmdd)	Time ± Error (hhmm:ss UT)	MLT (h)	Mlat (deg)
a	960814	0404:00 ± 120 s	22.3 ± 0.3	65
	960814	0413:00 ± 120 s	23.5 ± 0.5	65
b	970904	1105:52 ± 19 s	21.5 ± 0.3	67
	970904	1108:19 ± 18 s	24.0 ± 1.0	67
c	970930	0925:35 ± 18 s	21.5 ± 0.5	71
	970930	0936:37 ± 19 s	23.5 ± 0.2	68
d	980907	0234:50 ± 55 s	22.0 ± 0.2	67
	980907	0238:12 ± 37 s	22.7 ± 0.3	68
e	981103	0924:03 ± 37 s	22.8 ± 0.3	68
	981103	0928:39 ± 19 s	23.8 ± 0.2	70
f	011222	1746:24 ± 13 s	23.0 ± 0.3	66

ponent with its peak value of 800 km/s. At the first aurora onset at 0924 UT, Geotail detected flow reversal of $V_y \sim \pm 200$ km/s. Subsequently, Geotail started to detect the fast earthward flow at 0925 UT and reached its peak at 0928 UT. The second aurora occurred concurrently at 0928:39 UT ±19 s.

2.2. Analysis Results From Six Substorms

[18] For all six events, the Polar spacecraft acquired the global image of the aurora activity simultaneously with Geotail observations in the vicinity of the magnetic equator of the near-Earth tail. When Polar UVI data are not available, we use the data from the Polar VIS alternatively. Since the time resolution of the Polar UVI is higher, we visually inspected continuous time series data from the Polar UVI, so that the finest resolution of the onset time can be obtained.

[19] Table 1 lists the onset timings of the first and second auroras for six substorms. The determination of the first and the second auroras is the same as the procedures used for the event on 3 November 1998. The first aurora was chosen as the sudden intensification of aurora that occurred at the near-Earth dipolarization onset. When there was temporally and spatially separable intense auroral activity after the first one, we named the activity the second aurora. The error of the timings ranges from 13 s to 120 s, depending on intervals and integration times for auroral images. For the event on 14 August 1996 (event a), only the Polar VIS data are available, resulting in the error value of 120 s. Onset locations of auroral activities for the first and the second auroras are also given in Table 1. The error of the onset locations is given in MLT. This error is due to the spatial extent of the auroral spot (size of the bulge) seen in the image. Since active auroral bulge expands rapidly soon after its emergence, the error ranges from 0.2 to 1 h in MLT. The event on 22 December 2001 (event f) had relatively smaller auroral activity and had no noticeable second aurora onset.

[20] Figure 5 is the time series data of the magnetic field B_z and the ion velocity V_x in the GSM coordinate system together with the timings of auroral activations in Table 1. The time is scaled with universal time (UT). Figures 5a–5f correspond to the a–f events listed in Table 1. Each plot shows a 30 min interval of Geotail data of the near-Earth tail in the vicinity of the magnetic equator. The dipolarization signature was observed as the increasing feature of northward magnetic field B_z. The presence of fast earthward flows was observed as a positive increase of V_x as large as ~600 km/s. Red and blue crosses indicate the onset timings of auroral activations, where the vertical line is the center of the onset time and the horizontal line is the error. Two colors of crosses (red and blue) correspond to timings of auroral onsets (first and second, respectively).

[21] Let us focus on the timings of auroral activations. For the three events b, d, and e, the time lag between the first and the second auroras was ~4 min. The event e on 3 November 1998 was described in detail in the previous sections. This stepwise feature with the time lag of ~4 min timescale was also observed in events b and d. In the two events b and e, out of the three, the fast earthward flows were detected just before the second auroral onsets. For these two events b and e, the Geotail spacecraft was located in the same local time of the second aurora activations. The timings of the second aurora were coincident with the arrival of the fast earthward flow at the near-Earth tail. The result shows an association between the second aurora and the fast earthward flow both spatially and temporally, which is consistent with the idea that the second aurora was caused by the fast earthward flow for the events that had the second aurora ~4 min after the first aurora.

[22] The observed signatures and the detection of dipolarizations and plasma flows may differ greatly, depending on the measurement locations relative to the auroral activity. The relative locations between the auroral activity and the spacecraft locations will be discussed later with Table 2 and Figure 9. Roughly speaking, the tail observations for events a, d, e, and f are good conjunction with the substorm onset aurora (the first aurora). The azimuthal separations between the location of the substorm onset aurora and the location of Geotail were approximately 1 h for these four events. On the other hand, the tail observations for events b and c are poor conjunction with the substorm onset aurora.

[23] Figure 6 shows distribution of onset locations from aurora imager data. The locations are given in the magnetic local time (MLT) and the Mlat in Table 1. Figure 6 redraws the locations for the first aurora (red larger filled circle) and second aurora (blue smaller filled circle). Both first and second auroras initiated mostly in the premidnight sector. The location of the first aurora onsets are distributed from 21 to 23 h MLT, while that of the second aurora onsets are distributed from 23 to 24 h MLT. Figure 6b demonstrates relative locations between the first and second aurora onsets for each event. In Figure 6, we put the first aurora at 22 h MLT and 65° Mlat and used the first aurora location as the reference location to illustrate the second auroral onset location from the relative distance between the first auroral onset. It is seen that all second auroras were initiated eastward of the first aurora onset location.

3. Summary and Discussion

3.1. Synthesis for Substorm Event on 3 November 1998

[24] We discuss a potential scenario to explain the chronology of phenomena for the substorm event on 3 November 1998. The top of Figure 7 shows a schematic summary of the observations from Geotail and Polar. The observed timings are rounded within errors in UT just for simplicity. From the Geotail observations, there were three potentially relevant phenomena, the signature of the ballooning mode (0922 UT) [*Saito et al.*, 2008b], the detection of fast mode

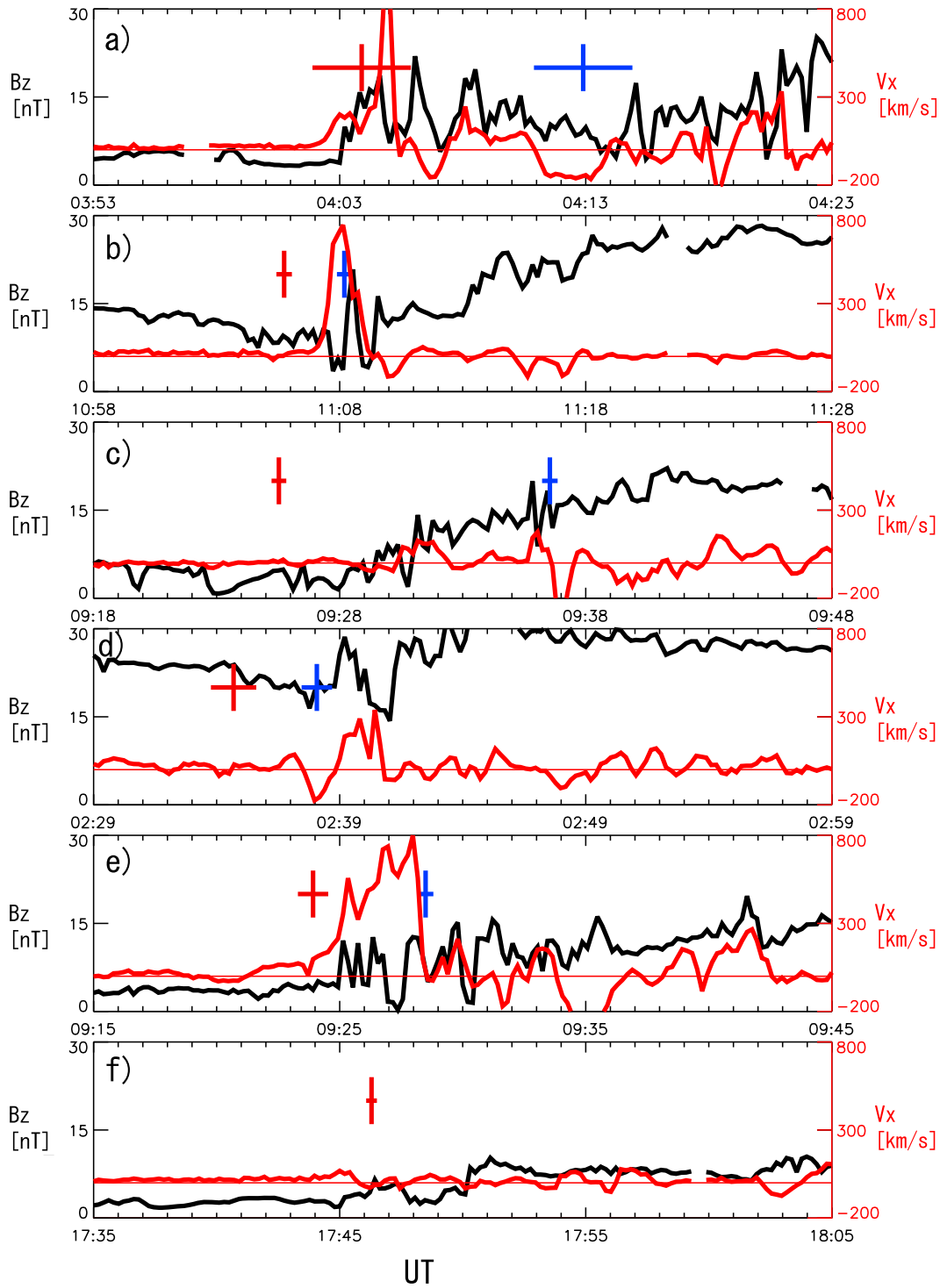

Figure 5. Geotail observations in the vicinity of the magnetic equator of the near-Earth tail, showing B_z (black line, left axis) and V_x (red line, right axis) of 6 dipolarizations as labeled as a–f in Table 1. Red (blue) crosses indicate the onset times of the first (second) aurora. The vertical and horizontal lines show the auroral onset time and the error, respectively.

waves propagating tailward (0923:30 UT) [*Saito et al.*, 2008a], and the detection of the fast earthward flow (0927 UT). From the Polar UVI data, there were two spatially and temporally separable auroral activations. The first aurora is the initial brightening of aurora, i.e., the substorm onset.

[25] The bottom of Figure 7 shows the synthesis constructed from the observations on 3 November 1998. The timings are given in relative time from the first aurora onset time (substorm onset time). The keys of observed timings are oriented as follows. First, one min prior to the first auro-

Table 2. Stepwise Aurora and Tail Processes[a]

Events	Date (yymmdd)	Stepwise Aurora (Within 2–6 min)	Fast Flow (V_x > 600 km/s)	Fast Wave	Ballooning Wave	Δ MLT (h)
a	960814		Y		Y	0.9
b	970904	Y	Y			3.0
c	970930				Y	2.6
d	980907	Y		Y		1.1
e	981103	Y	Y	Y	Y	0.6
f	011222				Y	−0.7

[a]Detections of the signatures are indicated with a letter Y. Δ MLT is the azimuthal separation between Geotail and the initial auroral brightening.

ra the near-Earth disturbance took place and launched the various waves. These disturbances included the fast mode waves that propagated perpendicular to the magnetic field line in the magnetic equatorial plane. The speed of the fast mode wave propagation was estimated to be ~400 km/s [*Saito et al.*, 2008a]. The ion acoustic speed is approximately 600 km/s calculated from the observed ion temperature of ~4 keV. Assuming the propagation speed of 400 km/s, the travel time from the near-Earth tail (X_{GSM} = −10 R_E) to the midtail (X_{GSM} = −20 R_E) is 160 s (~3 min). Three minutes after the near-Earth tail disturbance, which is two min after the first aurora onset, the magnetic reconnection occurs upon the arrival of the fast mode wave. The wavelength of the fast mode wave will be of the order of 5 R_E. The fast mode waves may play a role in compressing the wide range of the magnetotail simultaneously. This may provide a trigger of the magnetic reconnection that gives a rise to the fast plasma flows. The fast earthward plasma flow was observed in the near-Earth tail having the peak speed of 800 km/s. If the flow propagates with the constant flow velocity of 800 km/s during the passage from the midtail (X_{GSM} = −20 R_E) to the near-Earth tail (X_{GSM} = −10 R_E), the travel time is 1.5 min. Hence, at t = 3.5 min, the fast earthward flow brought kinetic energy to the near-Earth tail to cause the second aurora. After sufficient energy was transferred into the ionosphere in the form of Alfvén waves, the second aurora emerged at t = 4.5 min.

[26] The synthesis scenario is based on the following assumptions. First, the intense auroras are mapped to the near-Earth tail plasma sheet at X_{GSM} ~ −10 R_E. Second, we take the Alfvén transit time to be 1 min. This is actually a well accepted fact. In order to cause the intense aurora, a sufficient amount of energy needs to be transferred to the ionosphere. It is natural to consider that this energy to cause the intense aurora is carried by an Alfvén wave. Third, the fast mode waves must arrive at the midtail region and cause almost instantly the magnetic reconnection. This causality of

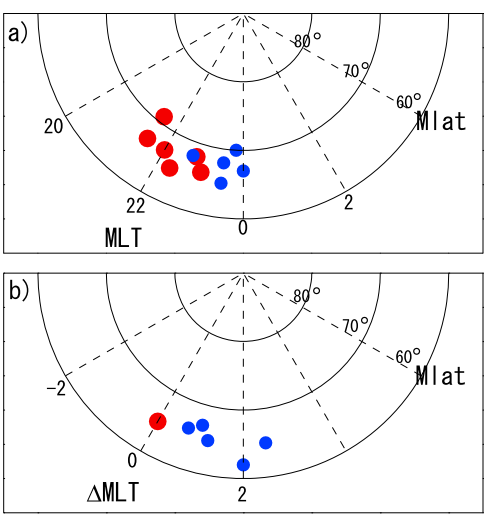

Figure 6. Distribution of the first aurora locations (red solid circles) and the second aurora locations (blue solid circles). (a) Locations in the AACGM coordinate system and (b) relative locations of the second aurora with respect to the first one.

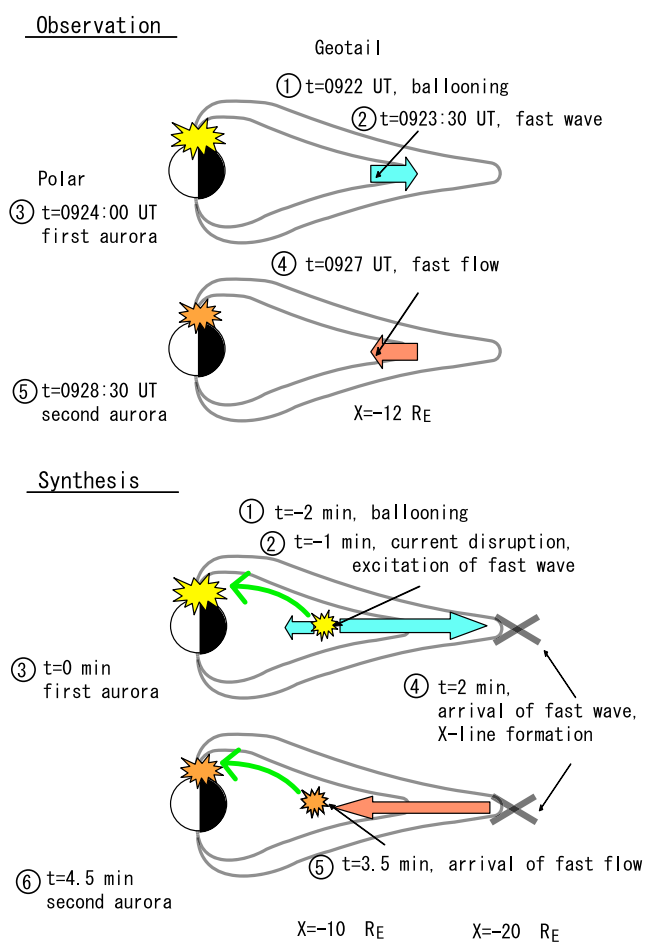

Figure 7. Summary of observations and synthesized scenario for the substorm event on 3 November 1998. The timings are rounded within errors for simplicity of presentation.

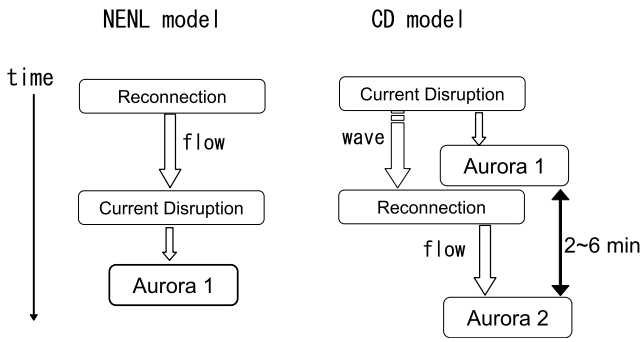

Figure 8. Surmised consequences of tail processes and associated auroral activity for two common models, the near-Earth neutral line (NENL) model and the current disruption (CD) model.

processes might be questionable. However, no study explains what is responsible for the initiation of the magnetic reconnection. The presence of the fast mode waves can be a hint for the potential trigger of the magnetic reconnection in the midtail. The validity of these assumptions requires further study. Since the observed timings were well explained by the scenario in Figure 7, the above considerations tentatively suggest observational constraints on substorm dynamics.

3.2. Conventional Substorm Models

[27] There are two phenomenological scenarios that stand widely accepted in the substorm community. The two opposed scenarios are called the near-Earth neutral line model and the current disruption model, and differ in its initial process in the tail. The two opposed scenarios include manifestations of substorm expansion signatures, namely, magnetic reconnection, plasmoid formation, and dipolarization (current disruption). Recently, these terms are comprehensively known as "outside-in" and "inside-out" models, respectively. For the background and the detail, see reviews [e.g., *Erickson*, 1995; *Lui*, 2001; *Ohtani*, 2004]. The modern version of both models agrees about the locations of the tail dynamics: An auroral substorm onset arc is mapped to the inner plasma sheet at $X_{\mathrm{GSM}} = -6$ to -10 R_E [*Samson et al.*, 1992]; the neutral line formation in the midtail at $X_{\mathrm{GSM}} = -15$ to -30 R_E [e.g., *Nagai et al.*, 1998; *Petrukovich et al.*, 1998; *Machida et al.*, 1999; *Miyashita et al.*, 2003; *Miyashita et al.*, 2009].

[28] Both models are based on the idea that there are two important key regions in the plasma sheet, the midtail and the near-Earth tail. The difference between these two models is the chronological order of the plasma processes in the central plasma sheet. The NENL model claims that the magnetic reconnection takes place before current disruption. Accordingly, the first activation of an aurora is caused by the earthward flow produced by magnetic reconnection after the flow reaches the near-Earth tail. The expansion scenario of the CD model [*Lui*, 1991] and the "inside-out" group of models requires a more complicated chain of processes. In order to account for the magnetic reconnection and the plasmoid formation, the disturbance due to the current disruption must propagate tailward. As a result, the fast earthward flow is generated to propagate to the near-Earth tail.

[29] Note that both models are phenomenological scenarios that are aimed to put the observed tail signatures into one framework, particularly into the framework of the magnetotail dynamics. Both models are not capable of explaining the detailed auroral behaviors. The question of how these models can explain auroral behaviors during substorm is far from solved.

3.3. Stepwise Aurora and the Models

[30] The dynamics that we interpreted in Figure 7 is fundamentally similar to those previously proposed for the "inside-out" group of substorm initiation models. The main difference between the synthesis in Figure 7 and the previously proposed scenario [e.g., *Friedrich et al.*, 2001] is the explicit addition of the second aurora that initiated with localized intense activity presumably caused by the arrival of the fast earthward flow at the near-Earth tail. It should be mentioned that similar scenarios have been repeatedly proposed, but this substorm event is the first observation that showed the presence of the ballooning mode wave, tailward propagating fast mode waves, and the timings of the second auroras from global images and the timings of the fast earthward flow. In particular, detailed inspection of the global auroral images enabled us to notice that the stepwise evolution during early substorm expansion phase onset is caused by the spatially and temporally different auroral activations that started locally, having different spatial structure from the initial auroral brightening. Therefore, it became possible to compare temporal and spatial relationship between the second aurora and the tail activities explicitly.

[31] Figure 8 shows simplified pictures of the two common substorm onset models with some surmised consequences. For simplicity of presentation, we omit the detailed expressions in Figure 8 as follows: Both substorm models are represented by the same keywords, reconnection, current disruption, flow, and Aurora 1 in Figure 8. Here "reconnection" represents the magnetic reconnection that is responsible for the formation of the fast plasma flows and the plasmoid in the magnetotail. As a result of "reconnection," the intense aurora is caused by the generated fast earthward flow arriving at the near-Earth tail. The fast earthward flow is represented by "flow" in Figure 8, which is preceded by "reconnection." In terms of the NENL model description, the near-Earth disturbance called dipolarization or current disruption is caused by the fast earthward flows. In the current disruption model, "current disruption" means the near-Earth tail instability that is responsible for the intense aurora. The intense aurora that corresponds to substorm expansion phase onset in Figure 8 is named "Aurora 1." In Figure 8 and in the discussion below, we use "current disruption" to represent the near-Earth tail disturbance responsible for the cause of the "Aurora 1." Note that the potential causes of the "current disruption" are different for these two models. The CD model invokes the current disruption as an internally excited instability rather than an instability excited by the arrival or the propagated disturbance from the midtail disturbance. The assumed causes of the "reconnection" are different for these two substorm models.

[32] The terminology of both "current disruption" and "reconnection" are often confusing. In the substorm study, both terms are often used to explain the substorm onset (but not the mechanism), while these two terms are also used to

interpret and to describe field and particle signatures observed in the magnetotail. These two terms describe the resultant phenomenon of plasma instability, but do not represent the cause. In other words, the large magnetic field variations are observed and are consistent with the idea of the transverse current disruption. This type of event is named current disruption, but causes and mechanisms of this phenomenon are largely unknown. Likewise the cause of the magnetic reconnection in the midtail is an outstanding issue. However, these two terms, current disruption and reconnection, are useful to describe the phenomenological signatures and potential consequences.

[33] The schematic chart for the CD model in Figure 8 includes two additional keywords, "wave" and "Aurora 2." Since any sudden changes of the state, which is an expected consequence at substorm expansion phase onset, may produce various waves, it is well expected that the near-Earth tail disturbance caused by the "current disruption" will excite some waves. The potential presence and roles of the "wave" as shown in Figure 8 were introduced by *Lui* [1991] in an effort to synthesize two facts: The latitudinal location of the initial auroral brightening and the magnetic reconnection pictures. Recent observational study from Geotail spacecraft in the vicinity of the plasma sheet showed the presence of the tailward propagating fast mode wave that had good temporal agreement with the initial auroral brightening [*Saito et al.*, 2008a]. In the following paragraph, we construct the surmised scenario for the CD model that includes "Aurora 2."

[34] Assuming the "wave" in Figure 8 is the ion acoustic wave, we obtain the specific time lag of 2–6 min between Aurora 1 and Aurora 2 as follows. The ion acoustic wave from the near-Earth tail ($X_{\mathrm{GSM}} = -10\ R_E$) propagates to the midtail ($X_{\mathrm{GSM}} = -20\ R_E$) with an ion acoustic speed of 500 km/s. Approximately 1 min (Alfvén transit time) after the current disruption that launches the sound wave, the intense aurora ("Aurora 1") appears. Here the sound wave is chosen, since the CD model expects a plasma instability in the magnetic equator where the absolute value of the magnetic field is small. The ion acoustic speed V_s is given by $V_s^2 = \gamma P_0/m_i n_0$, where γ, P_0, m_i, and n_0 are the constant of specific heat, the plasma pressure, the mass of ion, and the number density of ions, respectively. The approximate expression, in the Earth's plasma sheet, for the sound speed is given by $V_s \sim 309.3 \times \sqrt{T_i}$ km/s, where T_i is given in keV. Hence the typical value of the ion acoustic speed is of the order of 500 km/s. The plasma flow will come from the midtail at the speed of approximately 800 km/s. When the plasma flow reaches the near-Earth tail, the associated disturbance will cause the intense aurora ("Aurora 2") approximately after 1 min (Alfvén transit time). The range of 2–6 min for the time lag are calculated from the range of the midtail location from $X_{\mathrm{GSM}} = -15\ R_E$ to $X_{\mathrm{GSM}} = -25\ R_E$ by fixing the other values as described above.

[35] The fast mode wave speed of 500 km/s might be underestimated. Under the presence of the larger magnetic field, the expected group velocity of the fast mode wave should be larger, while Geotail detected small value of the ambient magnetic field, where the plasma β is of the order of 50. In this case, the speed of the fast mode wave becomes the order of the speed of the ion acoustic wave. Inside the neutral sheet, the expected value of the ambient magnetic field is also smaller and decreases away from the Earth. For the propagation inside the X-Y plane of the central plasma sheet, the speed of the fast wave is most likely to be of the order of the ion acoustic wave, which is determined only by the ion temperature and is not affected by the magnetic field. However, since our aim is to examine the causal relationship, the underestimate of the wave speed (i.e., overestimate of the time delay) will not cause much defect for estimating the expected range of time lag.

3.4. Possible Types of Substorm Dynamics

[36] For event a on 14 August 1996, the fast earthward flow was detected by Geotail, coinciding with the first aurora activation timing. Geotail was located in the same local time of both aurora activations. In this event, the auroral behaviors were different from the other five events. This substorm event was also documented and discussed by many authors [*Angelopoulos et al.*, 1999; *Frank et al.*, 2001; *Ohtani et al.*, 2002; *Yamaguchi et al.*, 2002]. The first aurora dimmed before the second aurora. The second activations occurred ~9 min after the first one. Event a is different from the case for events b, d, and e in terms of time lags. The time lag of 9 min conflicts with the prediction made for CD model in Figure 8. Therefore, event a may follow a different chain of processes than that outlined in Figure 8.

[37] Event f on 22 December 2001 is another event in which the auroral evolution was distinctly different from other events. Event f had no second aurora, but the auroral duration was longer (~20 min). In this event, Geotail was located in the same local time of the aurora and outside the strong dipole field region. The degree of the dipolarization was small having no significant ion flow observed. Event f conflicts with both models shown in Figure 8; therefore, an additional type of substorm is expected.

[38] Let us make some comments on the analysis of event c on 30 September 1997. It is not always easy to determine or differentiate second auroral activations from the Polar UVI data. This is partly due to the disturbed nature of the aurora during early expansion phase of substorms. Intensity of auroral distributions is not flat and varies with time in a fluctuating manner. In order to avoid artificial bias and confusions, we picked the second auroral onset and location when we could see them well separated from the first one. For this event, we picked the second auroral activation that occurred 11 min after the first one. However, there was actually a second aurora-like feature seen in the auroral images 3 min (0928:03 UT ±17 s) after the first one. The location of this feature was 22 ± 0.5 h in MLT and 71° in Mlat. Therefore, there is a possibility that event c can be placed in the same category as events b, d, and e in terms of the time lag of 2–6 min for the stepwise feature.

[39] Table 2 summarizes the observation results from this paper and our previous works [*Saito et al.*, 2008a, 2008b; *Saito*, 2008]. The detection of the fast mode wave was given in *Saito* [2008] by using two methods: One is estimating phase speed from magnetic field and velocity fluctuations, assuming a linear theory in low-frequency regime [*Saito et al.*, 2008a]. Another method is examining magnetic and plasma pressures. Both methods lead to the same result, namely the fast mode wave was found for events d and e at the time prior to dipolarization onset. The detection of the ballooning mode wave was shown in [*Saito et al.*, 2008b] by using wavelet analysis of the magnetic field vec-

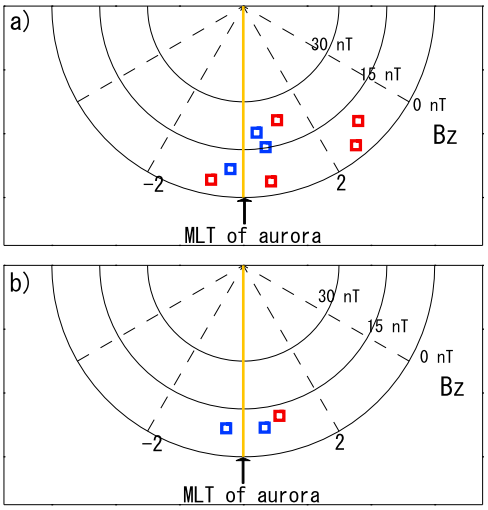

Figure 9. Locations of the Geotail spacecraft, when auroral onsets were observed (a) without and (b) with the fast earthward flow in the near-Earth tail. The spacecraft locations are plotted in the relative magnetic local time and B_z magnitude. The colors (red and blue) are the same as for Figure 6.

tor. The wavelet analysis yields azimuthal propagation of low-frequency wave. The wavelengths were estimated using ion velocity measurements and were found to be of the order of ion gyroradius, which is expected from the kinetic and fluid theories.

[40] For convenience of discussion below, we define stepwise aurora. When the time lag between the first and the second aurora onsets is in the range of 2–6 min, we regard this type of auroral evolution as stepwise aurora. Events, such as event a, are not considered as stepwise aurora because when the time span between two auroras are larger than 6 min, it is uncertain whether there is causality between the two phenomena. The letter "Y" represents the detection of phenomena: stepwise aurora with 2–6 min timescale, fast earthward flow, fast mode wave, and ballooning mode wave.

[41] The azimuthal distance between Geotail and the first aurora ΔMLT varies from 0.6 to 3.0 h. When the distance was smallest (event e) and the auroral features were stepwise, Geotail observed all of them. Similarly in event d, the distance was small and the auroral feature was stepwise. Geotail also observed the fast mode wave; however, it failed to detect any fast earthward flows or the ballooning mode wave. This can be explained by the spacecraft location of Geotail. In event d, Geotail was located in the strong dipole field that can be seen in the value of ambient $B_z > 15$ nT. In contrast to events e and d, event b is the case when the distance was largest and the auroral feature was stepwise. In this case, Geotail detected the fast earthward flow, while it failed to detect ballooning mode signature and fast mode waves. Even though the spacecraft is located in the vicinity of the magnetic equator of the near-Earth tail, it may detect different magnetotail dynamics, depending on its azimuthal separation from the aurora and the strength of the dipole field (the radial location). The detection of the fast mode waves may be influenced by the inhomogeneous nature of the plasma sheet.

[42] Figure 9 shows Geotail locations when the first and the second aurora onsets occurred according to cases in which Geotail observed no significant earthward flow (Figure 9a) and observed the fast earthward flow (Figure 9b). The spacecraft locations are presented by squares. The colors red and blue correspond to the Geotail locations for the first aurora and the second aurora cases, respectively. The Geotail locations are plotted in the relative magnetic local time from the aurora onset and in the amplitudes of magnetic component B_z. Here the magnitude B_z in Figure 9 is a 5 min average around the auroral onset time.

[43] From Figure 9b, we can see that when Geotail detected the fast earthward flows, the spacecraft was located in the weak B_z regions in the magnetotail. Here the weak B_z region means that it is outside the strong dipole field so that the fast earthward flow can reach the near-Earth tail without much deceleration. Also we can see that there was the auroral brightenings that are located longitudinally near the fast earthward flow. The fast earthward flow is known to be associated with localized auroral activities [*Sergeev et al.*, 1999; *Zesta et al.*, 2000; *Nakamura et al.*, 2001]. While there is a close association between the fast earthward flows and the auroral onsets (both first and second), not all auroral onsets showed the association with the fast flow. From Figure 9a, we can see that there is the case when Geotail was very longitudinally near the aurora onsets and also was in the weak B_z region, but did not detect the fast earthward flow.

[44] Our six dipolarization events showed different tail signatures corresponding to the different types of stepwise auroral evolutions. The observed time lag was ~4 min for events b, d, and f and was ~10 min for events a and c. The former time lag insinuates that there is a causal relationship between the first and the second auroras, as described in section 3.3. The event f on 22 December 2001, in which there was no noticeable second aurora, can be understood as a case of the near-Earth disturbance generating the initial brightening, but failing to cause magnetic reconnection to produce the fast earthward flow, so that the second stage was not completed. In event a on 14 August 1996, in which the fast flows presumably generated the first aurora, the fast flow did not cause larger expansion of the aurora [*Ohtani et al.*, 2002].

[45] We interpreted these observations as showing at least three types of substorm expansion phase onset and corresponding auroral evolutions. Figure 10 shows our interpretations of substorm types speculated from this study of six substorms: type A, type A′, and type B. Here type A is exactly the same as the modules of the CD model in Figure 8. Events (b, d, and e) are categorized into type A, since their auroral evolutions had stepwise characteristics within 2–6 min. Also the near-Earth tail observations of the fast earthward flows were consistent with the scenario of type A. Here type A′ is a case when the aurora did not show stepwise characteristics nor the second aurora intensification (event f). In addition to this auroral difference, the fast earthward flow was not observed even though Geotail was almost in the same local time as the auroral brightening with the small northward magnetic field region within the central plasma sheet. Type B is a case when the fast earthward flow was observed concurrently with the first aurora (event a),

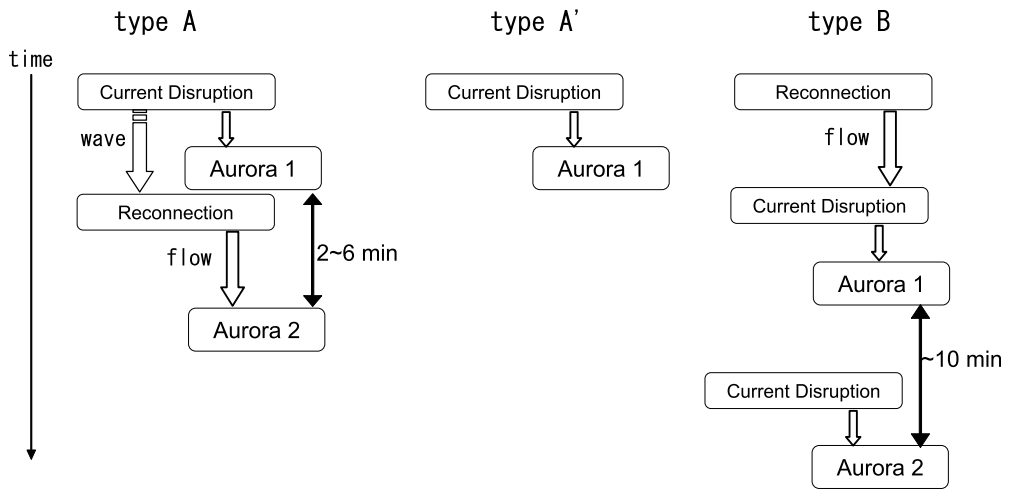

Figure 10. Types of substorm expansion phase onset. The key chain of processes relevant to the auroral activity are summarized with the simplified representations; see the text.

though the controlling factor for the second aurora onset with the time separation of ~10 min is unknown.

[46] In order to have consistency with other substorm studies, it should be mentioned that the first aurora for events a and f can be better categorized as pseudosubstorm events. In this study, we avoided categorizing dipolarization events into substorm and pseudosubstorm, since the goal of this study is to understand the magnetospheric physics behind the stepwise auroral evolutions. Furthermore, it is also controversial issue how to determine pseudosubstorm from full substorm events. Combining our results with the recent auroral study by *Rae et al.* [2009], it may be speculated that an auroral activation event with a lack of the stepwise feature within 2–6 min or a lack of N–S aurora will be classified as pseudobreakup event.

[47] For event a, the first aurora was named pseudo-onset by *Frank et al.* [2001] and *Ohtani et al.* [2002], while *Angelopoulos et al.* [1999] categorized this as a classical substorm on the basis of ground-based magnetic field showing low-to-high latitude development. We speculate the possible consequences as shown in Type B, which is different from the NENL model in a way that fast flow does not necessary cause current disruption in a large scale [*Ohtani et al.*, 2002]. We separated the flow and the current disruption. In addition to that, a possibility that the second aurora was also caused by flow can be eliminated as follows. Geotail (23.2 h MLT) was located between the azimuthal location of the first (22.3 MLT) and the second (23.5 h MLT) aurora onsets, but did not detect any signature of fast flow in a region of the average B_z strength of 10 nT. Let us emphasize that type B model is preliminary and needs to be studied further using better auroral observations with finer temporal and spatial resolutions. Still we are confident with that Event a is different class of phenomena in terms of the stepwise feature of the aurora and the fast flow timings in the conjugate near-Earth tail observation.

3.5. "Stepwise" Feature of Auroral Expansion

[48] There is surprising consistency between our results and the statistical characteristics of the westward traveling surge and the persistent aurora features reported by *Craven et al.* [1989]. They used imager data on board Dynamic Explorer 1 to investigate behaviors of the auroral substorm associated with a westward traveling surge. They note that there was spatial and temporal separation between the westward traveling surge and the subsequent intense auroras at midnight; the average separation distances were approximately 700 km, ~1.2 h in MLT; the average times for the stepwise advance were approximately 5 min. These values are very close to what we obtained: the separation distances between the first and the second aurora onsets were 2.5 ± 1, 0.7 ± 0.3, and 1.0 ± 0.3 h in MLT for events b, d, and e, respectively. The events (b, d, and e) are substorms that showed the stepwise feature within 2–6 min. Taking into account the fact that there are auroral substorms that have the absence of the westward traveling surge signature [*Craven and Frank*, 1987], we may speculate that substorms with stepwise features within ~4 min belong to the same category of substorms that have a westward traveling surge and the persistent intense auroral activity. The spatial structure of the first aurora for event e (top of Figure 3) also shows spatial characteristics of a westward traveling surge [*Kamide and Akasofu*, 1975; *Gelpi et al.*, 1987; *Craven et al.*, 1989; *Nakamura et al.*, 1993]. Because the stepwise feature observed in this study may be difficult to identify from ground-based all-sky cameras, an identification of a westward traveling surge may be used to categorized auroral substorms. In addition to that, the second aurora is likely to be the same auroral phenomenon known as the N–S aurora that appeared eastward of the auroral bulge, while the westside of the bulge showed the signature of the westward traveling surge [*Nakamura et al.*, 1993]. *Nakamura et al.* [1993] suggested that the N–S aurora is possibly linked with the subsequent development of pulsating and diffuse auroras.

3.6. Future Works Using THEMIS Data

[49] Multipoint measurements in the magnetotail with concurrent auroral data are useful for understanding the substorm physics and are now available through NASA's magnetospheric mission Time History of Events and Macroscale Interactions during Substorms (THEMIS) [*Angelopoulos*,

2008; *Frey et al.*, 2008; *Mende et al.*, 2008]. The results from THEMIS, however, have not yet brought general agreement on the problem of substorm onset. The discussion as of now seems to focus on the issue of whether an expansion is initiated in the near-Earth tail or in the midtail regions.

[50] As proposed in the NENL model [*Hones and Schindler*, 1979], it is widely accepted that magnetic reconnection in the magnetotail plays some role during substorm expansion [e.g., *Sergeev et al.*, 2008]. A few min prior to an initial brightening of an aurora, THEMIS in the midtail detected small-amplitude fluctuations of magnetic field and plasma [*Angelopoulos et al.*, 2008]. The authors interpreted the observed fluctuation to be related to the magnetic reconnection (see comment on this paper by *Lui* [2009]). However, the problem of how magnetic reconnection, or reconfiguration of the magnetotail, can cause the sudden intensification of aurora and the subsequent development is far from solved.

[51] The ballooning instability [*Roux et al.*, 1991] has been discussed as a likely mechanism of substorm expansion onset. There are several observational reports on aurora in favor of ballooning instability [*Donovan et al.*, 2007; *Liang et al.*, 2008; *Henderson*, 2009]. However, we should bear in mind that the low-frequency wave is not sufficient for a substorm onset but the process involves high-frequency waves as well [e.g., *Lui et al.*, 2008a; *Liang et al.*, 2009]. Tentative theories have been proposed to account for the behaviors of high-frequency waves observed in the near-Earth tail region [*Lui et al.*, 2008b; *Liu and Liang*, 2009]. Careful consideration is required to conclude the role of the ballooning instability in the substorm expansion mechanisms.

[52] Before addressing and concluding substorm expansion physics and onset mechanisms, it is worth answering the more fundamental problem of how aurora and magnetotail dynamics are related. Since the two-stage expansion observed here has a characteristic separation of 4 min and 1–2 R_E in the magnetotail, THEMIS can separate the spatial and temporal differences of the tail signatures depending on location and stage. Careful analyses of THEMIS data with the two-stage aspect may provide the relationship between the aurora and magnetotail and therefore lead to the observational constraints necessary for a theoretical model of substorm expansion. Using the fact that intense auroral activity can be spatially and temporally separable, we can reveal the relationship between magnetotail and auroral activities that include not only initial brightening but also prior and post activities.

4. Conclusions

[53] We studied the stepwise feature of auroral evolution at substorm expansion phase onset by examining the six substorms using simultaneous observations of aurora and the near-Earth tail using Polar and Geotail data, respectively. The observation on 3 November 1998 showed that the auroral activity consisted of the initial brightening and subsequent intense auroral activity with the time delay of 4.5 min. The stepwise features of auroral expansion were seen as two temporally and spatially separable intense auroral spots in the global auroral images from Polar UVI.

[54] We found that the stepwise feature (the second auroral onset) was found for five out of six events and were located eastward of the first auroral intensifications for all five cases. The time lag of ~4 min for the stepwise auroral evolution was a common feature for three out of six events. The time lag of ~4 min can be explained by the chain of processes in the central plasma sheet as advocated by *Friedrich et al.* [2001]. The two stages are presumably completed by a cause and effect relationship between the near-Earth instability and magnetic reconnection. If these two processes are linked by the tailward sound waves, the two intense auroras may occur with the characteristic time lag of 2–6 min.

[55] Our important result is that the tail processes associated with the second aurora are responsible for the significant expansion behavior of the auroral substorm. The substorm scenario interpreted for 3 November 1998 event and the stepwise feature within 2–6 min are essentially the same as the previously proposed CD models [*Lui*, 1991; *Friedrich et al.*, 2001]. The explicit representation of the second aurora in the substorm initiation scenario becomes possible owing to Polar UVI and VIS data with the concurrent and the conjugate near-Earth tail data. The auroral feature of the first aurora showed well-known features for the westward traveling surge which is frequently observed, or one of the most characteristic signatures of the auroral substorm onset [*Akasofu*, 1974]. Our observation on 3 November 1998 allowed us to compare the temporal and spatial characteristics of the second aurora with the conjugate near-Earth tail data. The timing of the arrival of the fast flow and the appearance of the second aurora was consistent with the idea that the second aurora is caused by the fast earthward flow that is presumably generated by the magnetic reconnection in the midtail. The magnetic reconnection just after the onset plays a key role in widening and spreading the auroral bulge. There are at least two different mechanisms operating during early stages of the substorm expansion phase for releasing the energy stored in the magnetotail. One occurs in the near-Earth tail which is responsible for triggering the substorm onset and is responsible for the formation of the westward traveling surge (first aurora); another is the magnetic reconnection, which is responsible for the formation of the N–S aurora (second aurora) and is responsible for the additional energy release processes during the substorm in a wide range of local time.

[56] The variations of the time lag suggest that there are at least three types of substorms that can be attributable to different tail processes, which can be discriminated by the time lag of the stepwise feature of the auroral expansion. In closing, we suggest that one way to resolve long-standing controversies on the substorm onset phenomenology is to categorize substorm events on the basis of physics-based quantities, such as the time lag as shown in this paper.

[57] **Acknowledgments.** The Geotail MGF magnetic field data were provided by S. Kokubun and T. Nagai. We thank G.K. Parks for providing the Polar UVI data. The data analysis systems for Polar VIS were supported in part at the University of Iowa by the National Aeronautics and Space Administration under NAG5-11528. The Polar VIS photographs were provided through CDAWeb at NASA. We thank A.T. Lui for helping with references for this work. This research is partly supported by the National Council of the Republic of China under grant NSC 97-2111-M-008-006-MY3 to National Central University.

[58] Wolfgang Baumjohann thanks the reviewer for his/her assistance in evaluating this paper.

References

Akasofu, S.-I. (1964), The dynamical morphology of the aurora polaris, in *Seismology*, *Ann. Int. Geophys. Year*, vol. 30, p. 300, Pergamon, New York.

Akasofu, S.-I. (1965), Dynamic morphology of auroras, *Space Sci. Rev.*, *4*, 498–540.

Akasofu, S.-I. (1972), Photographs of the front of the expanding auroral bulge during an auroral substorm, *Planet. Space Sci.*, *20*, 821–822.

Akasofu, S. I. (1974), A study of auroral displays photographed from the DMSP-2 satellite and from the Alaska meridian chain of stations, *Space Sci. Rev.*, *16*, 617–725.

Angelopoulos, V. (2008), The THEMIS mission, *Space Sci. Rev.*, *141*, 5–34, doi:10.1007/s11214-008-9336-1.

Angelopoulos, V., et al. (1996), Multipoint analysis of a bursty bulk flow event on April 11, 1985, *J. Geophys. Res.*, *101*, 4967–4989.

Angelopoulos, V., et al. (1999), On the relationship between bursty bulk flows, current disruption and substorms, *Geophys. Res. Lett.*, *26*(18), 2841–2844.

Angelopoulos, V., et al. (2008), Tail reconnection triggering substorm onset, *Science*, *324*(5933), 1391, doi:10.1126/science.1160495.

Baker, K. B., and S. Wing (1989), A new coordinate system for conjugate studies at high latitudes, *J. Geophys. Res.*, *94*, 9139–9143.

Blanchard, G., L. Lyons, J. Samson, and F. Rich (1995), Locating the polar cap boundary from observations of 6300 auroral emission, *J. Geophys. Res.*, *100*, 7855–7862.

Blanchard, G., L. Lyons, and J. Samson (1997), Accuracy of using 6300 Å auroral emission to identify the magnetic separatrix on the nightside of Earth, *J. Geophys. Res.*, *102*, 9697–9703.

Craven, J., and L. Frank (1987), Latitudinal motions of the aurora during substorms, *J. Geophys. Res.*, *92*, 4565–4573.

Craven, J., L. Frank, and S.-I. Akasofu (1989), Propagation of a westward traveling surge and the development of persistent auroral features, *J. Geophys. Res.*, *94*, 6961–6967.

Donovan, E., S. Mende, B. Jackel, M. Syrjäsuo, M. Meurant, I. Voronkov, H. Frey, V. Angelopoulos, and M. Connors (2007), The azimuthal evolution of the substorm expansive phase onset aurora, in *Proceedings of International Conference on Substorms-8*, edited by M. Syrjäsuo and E. Donovan, pp. 55–60, Univ. of Calgary, Calgary, Alberta, Canada.

Elphinstone, R., J. Murphree, and L. Cogger (1996), What is a global auroral substorm?, *Rev. Geophys.*, *34*, 169–232.

Erickson, G. M. (1995), *Substorm theories: United they stand, divided they fall*, *NASA-CR-197672*, NASA Goddard Space Flight Cent., Greenbelt, Md.

Frank, L. A., J. B. Sigwarth, J. D. Cravens, J. S. Dolan, M. R. Dvorsky, P. K. Hardebeck, J. D. Harvey, and D. W. Muller (1995), The visible imaging system (VIS) for the Polar spacecraft, *Space Sci. Rev.*, *71*, 297–398.

Frank, L. A., W. R. Paterson, J. B. Sigwarth, and T. Mukai (2001), Observations of plasma sheet dynamics earthward of the onset region with the Geotail spacecraft, *J. Geophys. Res.*, *106*, 18,823–18,841.

Frey, S., V. Angelopoulos, M. Bester, J. Bonnell, T. Phan, and D. Rummel (2008), Orbit design for the THEMIS mission, *Space Sci. Rev.*, *141*, 61–89, doi:10.1007/s11214-008-9441-1.

Friedrich, E., J. Samson, I. Voronkov, and G. Rostoker (2001), Dynamics of the substorm expansive phase, *J. Geophys. Res.*, *106*, 13,145–13,163.

Gelpi, C., H. Singer, and W. Hughes (1987), A comparison of magnetic signatures and DMSP auroral images at substorm onset: Three case studies, *J. Geophys. Res.*, *92*, 2447–2460.

Henderson, M. G. (2009), Observational evidence for an inside-out substorm onset scenario, *Ann. Geophys.*, *27*, 2129–2140.

Hones, E., Jr. (1985), The poleward leap of the auroral electrojet as seen in auroral images, *J. Geophys. Res.*, *90*, 5333–5337.

Hones, E., Jr., and K. Schindler (1979), Magnetotail plasma flow during substorms: A survey with IMP 6 and IMP 8 satellites, *J. Geophys. Res.*, *84*, 7155–7169.

Hones, E., Jr., S. Bame, and J. Asbridge (1976), Proton flow measurements in the magnetotail plasma sheet made with Imp 6, *J. Geophys. Res.*, *81*, 227–234.

Kadokura, A., A.-S. Yukimatu, M. Ejiri, T. Oguti, M. Pinnock, and P. R. Sutcliffe (2002), Detailed analysis of a substorm event on 6 and 7 June 1989: 2. Stepwise auroral bulge evolution during expansion phase, *J. Geophys. Res.*, *107*(A12), 1480, doi:10.1029/2001JA009129.

Kamide, Y., and S.-I. Akasofu (1975), The auroral electrojet and global auroral features, *J. Geophys. Res.*, *80*, 3585–3602.

Kokubun, S., T. Yamamoto, M. H. Acuna, K. Hayashi, K. Shiokawa, and H. Kawano (1994), The Geotail magnetic field experiment, *J. Geomagn. Geoelectr.*, *46*, 7–21.

Lassen, K., J. R. Sharber, and J. D. Winningham (1974), The development of an isolated auroral substorm, *Eos Trans. AGU*, *56*, 1170.

Liang, J., E. F. Donovan, W. W. Liu, B. Jackel, M. Syrjäsuo, S. B. Mende, H. U. Frey, V. Angelopoulos, and M. Connors (2008), Intensification of preexisting auroral arc at substorm expansion phase onset: Wave-like disruption during the first tens of seconds, *Geophys. Res. Lett.*, *35*, L17S19, doi:10.1029/2008GL033666.

Liang, J., W. W. Liu, E. F. Donovan, and E. Spanswick (2009), In-situ observation of ULF wave activities associated with substorm expansion phase onset and current disruption, *Ann. Geophys.*, *27*, 2191–2204.

Liu, W. W., and J. Liang (2009), Disruption of magnetospheric current sheet by quasi-electrostatic field, *Ann. Geophys.*, *27*, 1941–1950.

Lui, A. T. Y. (1991), A synthesis of magnetospheric substorm models, *J. Geophys. Res.*, *96*, 1849–1856, doi:10.1029/90JA02430.

Lui, A. T. Y. (2001), Current controversies in magnetospheric physics, *Rev. Geophys.*, *39*(4), 535–563.

Lui, A. T. Y. (2009), Comment on "tail reconnection triggering substorm onset," *Science*, *324*(5933), 1391, doi:10.1126/science.1167726.

Lui, A. T. Y., et al. (2008a), Determination of the substorm Initiation region from a major conjunction interval of THEMIS satellites, *J. Geophys. Res.*, *113*, A00C04, doi:10.1029/2008JA013424.

Lui, A. T. Y., P. H. Yoon, C. Mok, and C.-M. Ryu (2008b), Inverse cascade feature in current disruption, *J. Geophys. Res.*, *113*, A00C06, doi:10.1029/2008JA013521.

Machida, S., Y. Miyashita, A. Ieda, A. Nishida, T. Mukai, Y. Saito, and S. Kokubun (1999), GEOTAIL observations of flow velocity and north–south magnetic field variations in the near and mid-distant tail associated with substorm onsets, *Geophys. Res. Lett.*, *26*(6), 635–638.

Mende, S. B., S. E. Harris, H. U. Frey, V. Angelopoulos, C. T. Russell, E. Donovan, B. Jackel, M. Greffen, and L. M. Peticolas (2008), The THEMIS array of ground-based observatories for the study of auroral substorms, *Space Sci. Rev.*, *141*, doi:10.1007/s11214-008-9380.

Meng, C.-I., and K. Liou (2002), Global auroral power as an index for geospace disturbances, *Geophys. Res. Lett.*, *29*(12), 1600, doi:10.1029/2001GL013902.

Miyashita, Y., S. Machida, K. Liou, T. Mukai, Y. Saito, H. Hayakawa, C.-I. Meng, and G. K. Parks (2003), Evolution of the magnetotail associated with substorm auroral breakups, *J. Geophys. Res.*, *108*(A9), 1353, doi:10.1029/2003JA009939.

Miyashita, Y., et al. (2009), A state-of-the-art picture of substorm-associated evolution of the near-Earth magnetotail obtained from superposed epoch analysis, *J. Geophys. Res.*, *114*, A01211, doi:10.1029/2008JA013225.

Mukai, T., S. Machida, Y. Saito, M. Hirahara, T. Terasawa, N. Kaya, T. Obara, M. Ejiri, and A. Nishida (1994), The low energy particle (LEP) experiment onboard the GEOTAIL satellite, *J. Geomagn. Geoelectr.*, *46*, 669.

Nagai, T., M. Fujimoto, Y. Saito, S. Machida, T. Terasawa, R. Nakamura, T. Yamamoto, T. Mukai, A. Nishida, and S. Kokubun (1998), Structure and dynamics of magnetic reconnection for substorm onsets with Geotail observations, *J. Geophys. Res.*, *103*, 4419–4440.

Nakamura, R., T. Oguti, T. Yamamoto, and S. Kokubun (1993), Equatorward and poleward expansion of the auroras during auroral substorms, *J. Geophys. Res.*, *98*, 5743–5759.

Nakamura, R., W. Baumjohann, R. Schodel, M. Brittnacher, V. Sergeev, M. Kubyshkina, T. Mukai, and K. Liou (2001), Earthward flow bursts, auroral streamers, and small expansions, *J. Geophys. Res.*, *106*, 10,791–10,802.

Oguti, T. (1975), Metamorphoses of aurora, in *Memoirs of the National Institute of Polar Research, Ser. A*, vol. 12, 101 pp., Natl. Inst. of Polar Res., Tokyo.

Ohtani, S. (2004), Flow bursts in the plasma sheet and auroral substorm onset: Observational constraints on connection between midtail and near-Earth substorm processes, *Space Sci. Rev.*, *113*, 77–96.

Ohtani, S., R. Yamaguchi, H. Kawano, F. Creutzberg, J. B. Sigwarth, L. A. Frank, and T. Mukai (2002), Does the braking of fast plasma flow trigger a substorm?: A study of the August 14, 1996 event, *Geophys. Res. Lett.*, *29*(15), 1721, doi:10.1029/2001GL013785.

Petrukovich, A., et al. (1998), Two spacecraft observations of a reconnection pulse during an auroral breakup, *J. Geophys. Res.*, *103*, 47–59.

Rae, I. J., et al. (2009), Timing and localization of ionospheric signatures associated with substorm expansion phase onset, *J. Geophys. Res.*, *114*, A00C09, doi:10.1029/2008JA013559.

Roux, A., S. Perraut, P. Robert, A. Morane, A. Pedersen, A. Korth, G. Kremser, B. Aparicio, D. Rodgers, and R. Pellinen (1991), Plasma sheet instability related to the westward traveling surge, *J. Geophys. Res.*, *96*, 17,697–17,714.

Saito, M. H. (2008), Observational studies of substorm initiation processes, Ph.D. thesis, Univ. of Tokyo, Tokyo.

Saito, M. H., Y. Miyashita, M. Fujimoto, I. Shinohara, Y. Saito, and T. Mukai (2008a), Modes and characteristics of low-frequency MHD waves in the near-Earth magnetotail prior to dipolarization: Fitting method, *J. Geophys. Res.*, *113*, A06201, doi:10.1029/2007JA012778.

Saito, M. H., Y. Miyashita, M. Fujimoto, I. Shinohara, Y. Saito, K. Liou, and T. Mukai (2008b), Ballooning mode waves prior to substorm-associated dipolarizations: Geotail observations, *Geophys. Res. Lett.*, *35*, L07103, doi:10.1029/2008GL033269.

Samson, J., L. Lyons, P. Newell, F. Creutzberg, and B. Xu (1992), Proton aurora and substorm intensifications, *Geophys. Res. Lett.*, *19*(21), 2167–2170.

Sergeev, V. A., and A. G. Yahnin (1979), The features of auroral bulge expansion, *Planet. Space. Sci.*, *27*, 1429–1440.

Sergeev, V. A., K. Liou, C.-I. Meng, P. T. Newell, M. Brittnacher, G. Parks, and G. D. Reeves (1999), Development of auroral streamers in association with localized impulsive injections to the inner magnetotail, *Geophys. Res. Lett.*, *26*(3), 417–420.

Sergeev, V. A., S. Apatenkov, V. Angelopoulos, J. P. McFadden, D. Larson, J. W. Bonnell, M. Kuznetsova, N. Partamies, and F. Honary (2008), Simultaneous THEMIS observations in the near-tail portion of the inner and outer plasma sheet flux tubes at substorm onset, *J. Geophys. Res.*, *113*, A00C02, doi:10.1029/2008JA013527.

Torr, M. R., et al. (1995), A far ultraviolet imager for the international solar-terrestrial physics mission, *Space Sci. Rev.*, *71*, 329–383.

Tsyganenko, N. A. (1995), Modeling the Earth's magnetospheric magnetic field confined within a realistic magnetopause, *J. Geophys. Res.*, *100*(A4), 5599–5612, doi:10.1029/94JA03193.

Voronkov, I. O., E. F. Donovan, and J. C. Samson (2003), Observations of the phases of the substorm, *J. Geophys. Res.*, *108*(A2), 1073, doi:10.1029/2002JA009314.

Yamaguchi, R., H. Kawano, S. Ohtani, K. Yumoto, T. Mukai, Y. Saito, and H. Hayakawa (2002), The timing relationship between bursty bulk flows and Pi2s at the geosynchronous orbit, *Geophys. Res. Lett.*, *29*(6), 1092, doi:10.1029/2001GL013783.

Zesta, E., L. Lyons, and E. Donovan (2000), The auroral signature of earthward flow bursts observed in the magnetotail, *Geophys. Res. Lett.*, *27*(20), 3241–3244.

M. Fujimoto and Y. Saito, Institute of Space and Astronautical Science, Japan Aerospace Exploration Agency, 3-1-1 Yoshinodai, Sagamihara, Kanagawa 229-8510, Japan.

K. Liou, Johns Hopkins University Applied Physics Laboratory, Laurel, MD 20723, USA.

Y. Miyashita, Solar-Terrestrial Environment Laboratory, Nagoya University, Furo-cho, Chikusa-ku, Nagoya, Aichi 464-8601, Japan.

M. H. Saito, Institute of Space Science, National Central University, 300 Jhongda Rd., Jhongli, Taoyuan, Taiwan. (msaito@jupiter.ss.ncu.edu.tw)

J. B. Sigwarth, NASA Goddard Space Flight Center, Greenbelt, MD 20771, USA.